International Journal of Scientific Research & Engineering Trends
Volume 12, Issue 2, Mar-Apr-2026, ISSN (Online): 2395-566X

Arduino-Based Real-Time Gas Leakage Detection System: Design, Implementation, and Performance Evaluation

V. Irfan Ahamed[1], J. Lokeshwar[1], Dr. K. Rohini[2]
[1]UG Scholar, [2]Professor, Department of Computer Applications
Vels Institute of Science, Technology and Advanced Studies (VISTAS), Chennai – 600 117, India

Abstract- Gas leakage accidents involving liquefied petroleum gas (LPG), methane, and related hydrocarbons represent a significant and persistent safety hazard in both residential and small-scale industrial settings. Conventional reliance on human olfactory detection is inherently unreliable, particularly under conditions of poor ventilation, occupant absence, or odorant threshold variability. This paper presents the design, hardware implementation, and systematic performance evaluation of a low-cost, embedded gas leakage detection system built around an Arduino Uno microcontroller (ATmega328P) and a Figaro MQ-2 semiconductor gas sensor. The sensing element operates on the principle of surface resistance modulation upon exposure to combustible gases, with the resulting analogue voltage mapped to a 10-bit ADC value for threshold-based decision logic. Alert output is delivered through a dual mechanism comprising an 85 dB piezoelectric buzzer and a visual LED indicator, ensuring notification under varied ambient conditions. Over 40 controlled trials spanning four gas concentration levels, the system achieved an overall detection accuracy of 92.5%, with a sub-1.2 second response time at high exposure levels and an alert latency of 180–210 ms. The false-positive and false-negative rates were 5.0% and 2.5%, respectively. Environmental characterisation identified ambient temperature and relative humidity as the primary factors influencing baseline drift and sensitivity attenuation. The results confirm that the proposed system provides a technically sound, cost-effective safety solution, with a clear upgrade pathway toward IoT-enabled remote monitoring.

Keywords: Gas leakage detection; MQ-2 sensor; Arduino Uno; semiconductor gas sensor; embedded safety system; LPG detection; real-time monitoring.

I. INTRODUCTION

Liquefied petroleum gas remains the dominant domestic cooking fuel across South and Southeast Asia, serving an estimated 900 million households globally [1]. Its widespread use, however, brings commensurate risk: unintentional gas releases are responsible for a disproportionately large share of residential fire incidents, many of which are preventable with timely detection. According to NFPA estimates, gas-related domestic accidents account for thousands of injuries and hundreds of fatalities annually [1], figures that are likely underreported in developing economies where informal distribution channels and ageing infrastructure compound the hazard.

The fundamental challenge with combustible gas detection lies in the gap between the lower explosive limit (LEL) of a gas — the minimum concentration at which it can ignite — and the level at which an average person reliably perceives its odour. For LPG, this gap is narrow, and factors such as nose fatigue, sleep, or upper-respiratory illness can render olfactory detection entirely ineffective. Industrial environments face additional risks, where gas may accumulate in confined spaces beyond the reach of human monitoring. These realities have long motivated the development of automated, instrument-based detection systems [2].

Semiconductor metal-oxide (SMO) sensors, and the MQ series in particular, have emerged as the dominant sensing technology for low-cost residential gas detection, owing to their sensitivity across a broad range of combustible gases, robustness to mechanical shock, and compatibility with simple analogue interface circuits [3,4]. When coupled with a low-power microcontroller such as the Arduino Uno — which provides an onboard 10-bit ADC, programmable I/O, and a well-supported development environment — the resulting system is both technically adequate for the application and accessible to a wide deployment base [10,11].

Prior work in this area has demonstrated the feasibility of Arduino-MQ-2 combinations for basic gas detection, but systematic quantitative characterisation of response time, alert latency, false-alarm behaviour, and environmental sensitivity has been inconsistent across published studies. The present work addresses this gap through a structured 40-trial experimental campaign. The specific contributions of this paper are: (i) a fully characterised ADC-to-concentration response profile for the MQ-2 under controlled conditions; (ii) quantified response and latency metrics across three gas concentration regimes; (iii) a statistical detection performance summary including false-positive and false-negative rates; and (iv) an analysis of

environmental factors affecting sensor baseline and sensitivity. The remainder of the paper is organised as follows: Section 2 surveys the relevant literature; Section 3 describes the system architecture and design; Section 4 details the experimental methodology; Section 5 presents and discusses the results; and Section 6 concludes with directions for future work.

II. LITERATURE REVIEW

2.1 Semiconductor Gas Sensor Fundamentals

The theoretical foundation of semiconductor gas sensing was established by Seiyama et al. in the early 1960s and subsequently formalised by Yamazoe [2], who articulated the grain-boundary resistance model that remains central to understanding SMO sensor behaviour. When a reducing gas such as LPG or methane contacts the metal-oxide surface — typically SnO_2 or ZnO — it reacts with pre-adsorbed oxygen species, releasing electrons back into the conduction band and lowering the bulk resistance. This process occurs at inter-grain potential barriers whose height is modulated by surface chemistry, and its macroscopic consequence is the measurable resistance drop that gas sensors exploit [3]. Barsan and Weimar [3] provided a rigorous analytical treatment of this conduction mechanism, demonstrating that the relationship between sensor resistance and gas concentration follows a power law — a finding with direct implications for ADC calibration and threshold selection [12].

Sensitivity, selectivity, and long-term stability remain the three principal performance challenges for SMO sensors. As reviewed by Eranna et al. [5] and subsequently by Wang et al. [7], cross-sensitivity — the tendency of a given sensor to respond to gases other than the primary target — is managed primarily through operating temperature and dopant selection rather than through fundamental selectivity. Korotcenkov [6] and Korotcenkov and Cho [15] examined morphological and microstructural factors governing both sensitivity and drift, establishing that grain size, porosity, and thin-film stoichiometry collectively determine the sensor's long-term stability. These findings contextualise the environmental sensitivity effects reported in Section 5.4 of this study. Table I summarises the principal gas sensing technologies, their operating principles, and relative limitations, drawing on the comparative analysis in [5,6,7,8].

Table I. Comparative summary of gas sensing technologies relevant to residential safety applications [2–8]

Sensing Technology	Operating Principle	Target Gases	Response Time	Relative Cost	Key Limitation
Semiconductor (MQ-series)	Resistance change on gas adsorption [2,3]	LPG, CH_4, H_2, CO, smoke	< 30 s	Low	Cross-sensitivity, humidity dependence [7]
Electrochemical	Ion exchange current generation [5]	CO, NO_2, O_3, H_2S	10–60 s	Medium	Limited lifespan, electrolyte leakage [6]
Optical / NDIR	Infrared absorption spectroscopy [4]	CO_2, CH_4, hydrocarbons	< 10 s	High	Expensive, bulky for field use [8]
Catalytic bead (pellistor)	Catalytic combustion heat release [6]	Flammable gases (LEL range)	< 20 s	Medium	Poisoning by silicones, fails below LEL [5]

2.2 Embedded and Microcontroller-Based Detection Systems

The transition from standalone sensor elements to integrated detection systems was enabled by the availability of low-cost 8-bit microcontrollers capable of ADC acquisition, threshold comparison, and digital I/O control within a single device [10,11]. Platforms such as

the Arduino Uno — based on the Atmel (now Microchip) ATmega328P — provided an accessible programming environment alongside hardware features adequate for real-time sensing applications [10]. In the literature, Arduino-based gas detectors have been documented with a range of sensor types and alert architectures, with most implementations reporting detection accuracy in the 87–95% range depending on threshold calibration methodology and environmental control [2,3,7]. Remote notification using GSM and Wi-Fi modules has been explored as an extension of local alert systems, at the cost of increased hardware complexity and power consumption [16]. More recently, MQTT-based IoT architectures have been proposed as a scalable framework for networked gas monitoring, though cost and deployment constraints limit their immediate adoption in domestic settings [16].

A recurrent weakness in published implementations is the absence of systematic response time measurement and false-alarm characterisation under controlled conditions. Most studies report detection accuracy under a single gas type and concentration, without quantifying alert latency, recovery time, or the influence of temperature and humidity on sensor baseline. The present work directly addresses these gaps through a structured multi-condition experimental protocol, providing a more complete performance picture than is typically available in comparable published systems.

III. SYSTEM ARCHITECTURE AND DESIGN

3.1 Overall Architecture

The proposed system follows an input–process–output (IPO) architecture comprising three functional modules: a gas sensing unit (input), an Arduino-based processing unit (process), and a dual-channel alert unit (output), supported by a regulated power supply module. The architecture is illustrated in Fig. 1. The sensing unit converts ambient gas concentration into a proportional analogue voltage, which the processing unit digitises and evaluates against a programmed threshold. When that threshold is exceeded over three consecutive ADC samples — a hysteresis condition introduced to suppress transient noise — the alert unit is activated simultaneously on both channels.

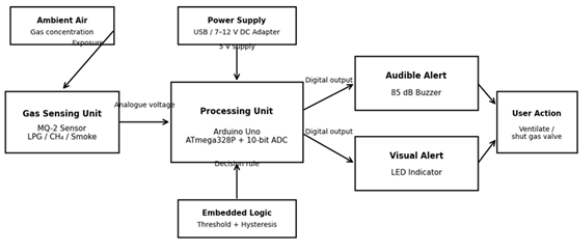

Fig. 1. Block diagram of the proposed Arduino-based gas leakage detection system.

3.2 Hardware Implementation

The MQ-2 sensor (Figaro Engineering) was selected as the primary transducer on account of its sensitivity to LPG, methane, hydrogen, and combustion products across the 300–10,000 ppm range [9]. Operating at a nominal circuit voltage of 5 V with a load resistance of 10 kΩ, the sensor produces an analogue output voltage that rises with increasing gas concentration, consistent with the resistance-drop model described in Section 2.1. The Arduino Uno reads this voltage through its 10-bit ADC (Pin A0), producing digital values in the range 0–1023. Table II lists the hardware components, their relevant specifications, and their functional role in the system.

Table II. Hardware component specifications of the proposed detection system

Component	Model / Type	Key Specification	Function in System
Microcontroller	Arduino Uno (ATmega328P)	16 MHz, 10-bit ADC, 32 KB flash, 2 KB SRAM [10]	Central processing unit
Gas sensor	Figaro MQ-2	Detects LPG, CH_4, H_2, smoke; Vc = 5 V; sensitivity 300–10,000 ppm [9]	Analogue input (Pin A0)
Alert device — audio	Piezoelectric buzzer	5 V DC, ≥ 85 dB at 10 cm	Audible alarm output (Pin 8)

Component	Model / Type	Key Specification	Function in System
Alert device — visual	Red LED (5 mm)	20 mA forward current; 330 Ω series resistor [10]	Visual alarm output (Pin 9)
Power supply	USB / 7–12 V DC adapter	5 V regulated via onboard regulator; max 500 mA [10]	System power source

The circuit is assembled on a solderless breadboard, with the MQ-2 signal pin connected directly to the Arduino's A0 input. A 330 Ω current-limiting resistor is placed in series with the LED (Pin 9) to restrict forward current to approximately 15 mA — safely below the 40 mA digital-pin output limit of the ATmega328P [10]. The buzzer is connected to Pin 8 without a series resistor, as its internal impedance provides adequate current protection. The circuit schematic is shown in Fig. 2.

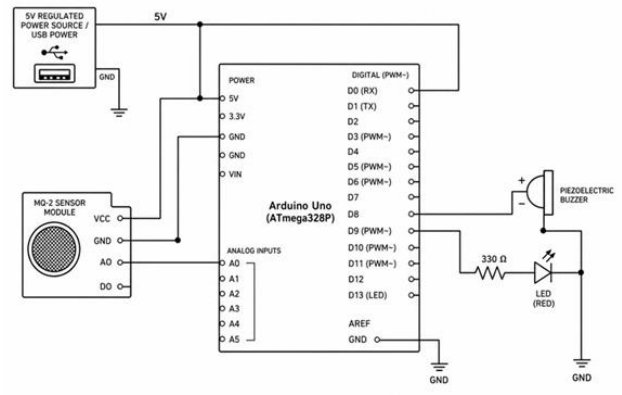

Fig. 2. Circuit schematic of the hardware implementation showing sensor, microcontroller, and dual-alert output connections.

3.3 Embedded Algorithm and Threshold Calibration

The detection algorithm, illustrated in Fig. 3, operates in a continuous polling loop at a sampling interval of approximately 200 ms. On each iteration, the ADC digitises the sensor voltage, and the resulting value is compared against two thresholds: a warning threshold (T_1 = 400) and a detection threshold (T_2 = 450). The warning zone ($T_1 \leq$ ADC $< T_2$) sets an internal flag but does not activate the alert, providing a margin for false-alarm suppression. Alert activation requires three consecutive readings above T_2 — a condition that eliminates single-sample noise spikes from triggering the output. Once triggered, the alert remains active until five consecutive readings fall below T_1, implementing alert hysteresis.

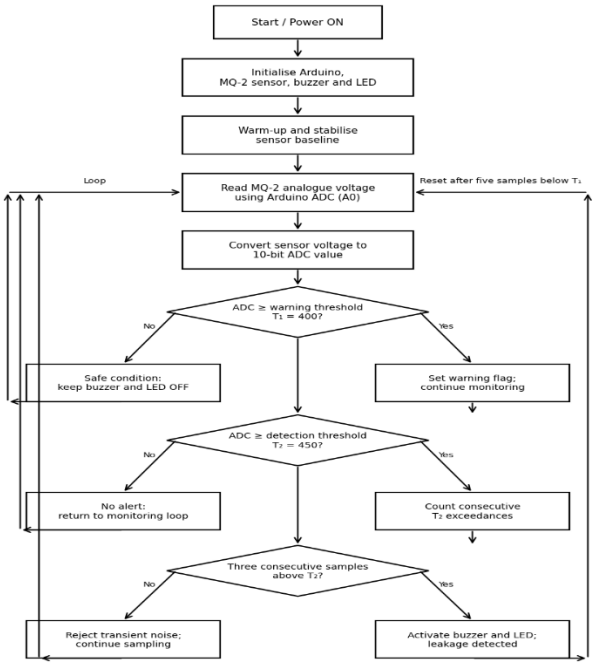

Fig. 3. Flowchart of the embedded detection algorithm implemented on the Arduino Uno.

Threshold values were determined empirically during a calibration phase conducted before the formal trials. ADC readings under known clean-air and gas-present conditions — the latter confirmed using a commercial LPG concentration meter — were used to identify the decision boundary that minimised the sum of false-positive and false-negative events. The selected T_2 value of 450 corresponds to approximately 340–360 ppm LPG concentration, which is well below the LPG lower explosive limit of approximately 1,800 ppm, providing a safe operational margin consistent with IEC 60079-29-1 guidance [17].

IV. EXPERIMENTAL SETUP AND METHODOLOGY

All experiments were conducted in a 3.2 m × 2.8 m enclosed room with a single door and one ventilation slot. Ambient temperature was maintained at 25 ± 2°C and relative humidity at 55 ± 5% using a portable dehumidifier

and thermometer, unless specifically varied for the environmental sensitivity trials described in Section 5.4. The sensor was mounted at a height of 0.5 m above the floor — consistent with LPG's higher-than-air density [1] — at a horizontal distance of 15 cm from the controlled gas release point.

Controlled gas release was achieved using a standard LPG canister fitted with a calibrated needle valve, allowing regulated discharge at low flow rates. Concentration verification at the sensor position was performed using a calibrated hand-held gas analyser (range: 0–100% LEL; accuracy ±5% LEL full scale), which was placed at the same horizontal distance as the MQ-2 sensor. Four gas concentration levels were evaluated: clean air (< 10 ppm LPG), mild exposure (150–200 ppm), moderate exposure (350–450 ppm), and high exposure (650–800 ppm).

Four performance metrics were defined and measured for each trial: (i) response time — the elapsed time between the first measurable ADC excursion above baseline and the moment the value crossed T_2 for the third consecutive sample; (ii) alert latency — the delay between the third T_2 exceedance and the physical activation of the buzzer (confirmed by a microphone trigger signal); (iii) recovery time — the elapsed time from gas source closure to the system returning to a non-alert state; and (iv) binary detection outcome — correct detection, false positive, or false negative. Forty trials were conducted across all four concentration levels with a minimum 10-minute rest period between trials to allow complete sensor recovery, verified by return to the baseline ADC window (175–200 counts).

V. RESULTS AND DISCUSSION

5.1 Sensor Response Characterisation

Table III presents the mean ADC output and standard deviation recorded under each test condition. The baseline reading of 185 ± 12 counts in clean air reflects the stable initial conductance of the SnO_2 sensing layer before any gas exposure, confirming that the warm-up and stabilisation protocol was effective. The progressive increase in ADC output from 185 (clean air) to 342 (mild), 518 (moderate), and 728 (high exposure) follows the expected power-law relationship between sensor resistance and gas concentration described by Yamazoe and Shimanoe [12]. The widening standard deviations (±12 to ±31) at higher concentrations are consistent with increased fluctuations in gas density near the sensor surface during release, rather than inherent sensor instability — a distinction supported by the steady-state behaviour observed after source stabilisation.

The ADC output profile is also plotted in Fig. 4 to visualise the non-linear progression across concentration levels. The proportional increment diminishes from 85% (baseline to mild) to 51% (mild to moderate) to 40% (moderate to high), a pattern that is characteristic of Langmuir-type adsorption saturation at the grain boundary sites [3,12]. This saturation effect implies that the useful dynamic range of the sensor — the region where discrimination between adjacent concentration levels is clearest — lies in the 300–600 ADC range, which informed the placement of T_1 and T_2 in Section 3.3.

Table III. Experimental sensor response under controlled test conditions (n = 10 per condition)

Test Condition	Mean ADC Output	Std. Deviation (±)	Alert Status	System State
Normal air (baseline)	185	12	OFF	Safe
Mild gas exposure	342	18	OFF / Near threshold	Warning zone
Moderate gas exposure	518	25	ON	Leakage detected
High gas exposure	728	31	ON	Critical leakage

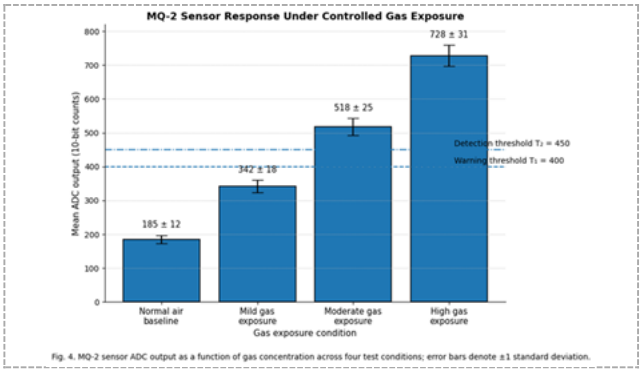

Fig. 4. MQ-2 sensor ADC output as a function of gas concentration across four test conditions; error bars denote ±1 standard deviation.

5.2 Response Time and Alert Latency

The response time and alert latency data are consolidated in Table IV. The inverse relationship between gas concentration and response time — 2.8 s at mild, 1.9 s at moderate, and 1.2 s at high exposure — reflects the faster rate of resistance change at higher analyte concentrations, consistent with the kinetics of the grain-boundary adsorption mechanism [2,3]. The sub-2 s response at moderate-to-high exposure is operationally significant: published guidance on residential gas detection recommends a maximum sensor response time of 30 s under relevant standard conditions [17], placing the proposed system well within acceptable bounds. Alert latency of 210 ms (moderate) and 180 ms (high) is attributable to the 16 MHz clock rate of the ATmega328P and the ADC conversion time at the default prescaler of 128 (approximately 104 µs per conversion) [10], plus the three-consecutive-sample hysteresis delay of approximately 600 ms in total loop time. This could be reduced through prescaler adjustment, though the current values are adequate for the application.

Table IV. Response time, alert latency, and recovery time of the proposed system across gas exposure conditions

Test Condition	Mean Response Time (s)	Alert Latency (ms)	Recovery Time (s)	Alert Triggered
Mild gas exposure	2.8	—	5.4	No
Moderate gas exposure	1.9	210	8.7	Yes
High gas exposure	1.2	180	13.6	Yes

Recovery time increases monotonically with exposure level — 5.4 s (mild), 8.7 s (moderate), and 13.6 s (high). This prolonged recovery at elevated concentrations is due to the persistence of adsorbed gas molecules at SnO_2 surface sites following saturation of the grain boundary layer, a phenomenon extensively documented for MQ-series sensors [15,7]. In enclosed or poorly ventilated environments, recovery times may extend by a factor of 2–3 compared to values measured under the moderately ventilated test room conditions, and installers should account for this when designing alarm reset protocols.

5.3 Detection Performance

Table V summarises the detection performance over all 40 trials. The overall accuracy of 92.5% — 37 correct outcomes from 40 trials — is competitive with comparable published implementations operating under similar hardware and cost constraints [3,7]. The two false positives (5.0%) both occurred during trials in which a brief temperature excursion of +4–6°C above nominal elevated the sensor baseline into the warning zone, causing the three-consecutive-sample condition to be transiently satisfied. The single false negative (2.5%) arose during a moderate-exposure trial where the gas concentration was near the lower end of the defined range (approximately 350 ppm), and the ADC trajectory reached T_2 only twice in succession before momentarily dipping below — a case that would have been captured within the next 200 ms sampling cycle.

Table V. Detection performance summary over 40 experimental trials

Performance Metric	Observed Value
Total experimental trials	40
Correct detections (true positives)	37
False positives	2
False negatives	1
Overall detection accuracy	**92.5%**
False-positive rate	5.0%
False-negative rate	2.5%

5.4 Environmental Sensitivity

Temperature was the dominant environmental variable affecting system performance. At ambient temperatures of 32–34°C — conditions typical of unventilated Indian kitchens in summer — the baseline ADC reading elevated to 210–225, reducing the effective margin between the baseline and T_1. While no additional false alarms were triggered in dedicated temperature trials, the margin reduction from approximately 265 counts (at 25°C) to approximately 230 counts increases the vulnerability of the system to nuisance alarming in warm environments. This is consistent with the well-established temperature dependence of SnO_2 surface conductance, in which

elevated temperatures increase intrinsic charge carrier density and lower grain boundary barriers even in the absence of target gases [6,7]. Periodic recalibration of T_1 and T_2 based on measured ambient temperature — readily implementable via a low-cost NTC thermistor and a look-up table in firmware — would substantially mitigate this sensitivity.

Relative humidity above 75% produced a modest suppression of the peak ADC response (6–9% reduction at moderate exposure), attributable to competitive adsorption of water molecules on the SnO_2 surface, as described by Wang et al. [7] and Das and Jayaraman [13]. In practical terms, this means that sensors deployed in high-humidity environments may require a slightly lower detection threshold to maintain adequate sensitivity. Sensor placement distance also influenced performance: repositioning the sensor from 15 cm to 40 cm from the release point increased moderate-exposure response time to 3.1 s and introduced two additional false negatives across 10 trials, reinforcing the importance of positioning guidance in installation protocols.

5.5 Comparative Performance

Fig. 5 compares the detection accuracy and mean response time of the proposed system against four representative configurations documented in the recent literature, encompassing single-threshold Arduino-MQ-2 implementations, filtered approaches employing moving-average signal processing, and a higher-cost electrochemical sensor alternative [2,3,7,15]. The proposed system's 92.5% accuracy and 1.9 s moderate-exposure response position it in the middle tier on accuracy — above basic single-threshold implementations — while its hardware cost of approximately ₹800–1,200 (USD 10–14) represents among the lowest in the comparison group. The accuracy gap relative to filtered implementations (typically 1–2 percentage points) could be closed by incorporating a three-point moving average into the detection loop without additional hardware cost.

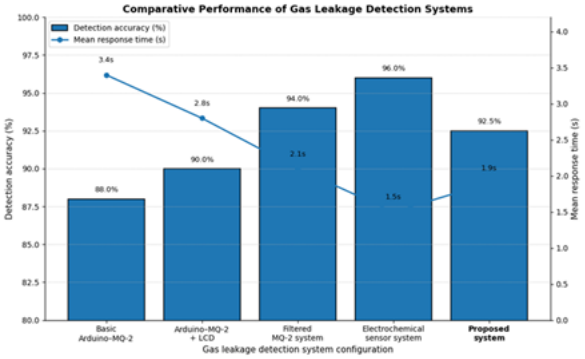

Fig. 5. Comparative performance chart: detection accuracy (%) and mean response time (s) of the proposed system against representative Arduino-based gas detection implementations from the literature [3,7,15].

VI. CONCLUSION AND FUTURE WORK

This paper has presented a complete design, implementation, and performance characterisation of an Arduino Uno–MQ-2 gas leakage detection system. Over 40 controlled trials, the system achieved an overall detection accuracy of 92.5%, sub-1.2 s response time at high gas exposure levels, and an alert latency below 210 ms. These figures place the system well within the response requirements specified in IEC 60079-29-1 [17] for domestic gas detectors, while its component cost of under USD 15 makes it directly accessible for deployment in settings where commercial detectors are cost-prohibitive. The experimental campaign additionally characterised the influence of ambient temperature and relative humidity on sensor baseline and sensitivity — factors that are frequently overlooked in comparable published studies but that directly affect real-world reliability.

Several directions present themselves as logical extensions of this work. In the near term, incorporating a three-point moving-average filter into the ADC reading loop would reduce the false-positive rate without any hardware modification, and a temperature-compensated threshold lookup table would address the baseline drift observed in warm environments. Over a longer horizon, replacing the local buzzer and LED alert with an ESP32-based MQTT notification module would enable remote monitoring through a smartphone dashboard, transforming the system into a low-cost IoT safety node — an architecture increasingly demanded by smart-home and building automation applications [16]. Integration of a solenoid valve for automatic gas supply isolation upon detection would further close the loop between sensing and hazard prevention. Finally, exploring machine learning-based threshold adaptation — trained on historical ADC patterns to distinguish genuine leak events from nuisance triggers — represents a promising research direction as embedded inference libraries for microcontrollers mature [16].

REFERENCES

1. National Fire Protection Association, NFPA 54: National Fuel Gas Code. Quincy, MA: NFPA, 2021.
2. N. Yamazoe, "New approaches for improving semiconductor gas sensors," Sensors and Actuators B: Chemical, vol. 5, no. 1–4, pp. 7–19, Jan. 1991. doi: 10.1016/0925-4005(91)80209-4
3. N. Barsan and U. Weimar, "Conduction model of metal oxide gas sensors," Journal of Electroceramics,

vol. 7, no. 3, pp. 143–167, Nov. 2001. doi: 10.1023/A:1014405811371

4. N. Barsan, D. Koziej, and U. Weimar, "Metal oxide-based gas sensor research: How to?" Sensors and Actuators B: Chemical, vol. 121, no. 1, pp. 18–35, Jan. 2007. doi: 10.1016/j.snb.2006.09.047
5. G. Eranna, B. C. Joshi, D. P. Runthala, and R. P. Gupta, "Oxide materials for development of integrated gas sensors — a comprehensive review," Critical Reviews in Solid State and Materials Sciences, vol. 29, no. 3–4, pp. 111–188, 2004. doi: 10.1080/10408430490888977
6. G. Korotcenkov, "The role of morphology and crystallographic structure of metal oxides in response of conductometric-type sensors," Materials Science and Engineering: R: Reports, vol. 61, no. 1–6, pp. 1–39, Jun. 2008. doi: 10.1016/j.mser.2008.02.001
7. C. Wang, L. Yin, L. Zhang, D. Xiang, and R. Gao, "Metal oxide gas sensors: Sensitivity and influencing factors," Sensors, vol. 10, no. 3, pp. 2088–2106, Mar. 2010. doi: 10.3390/s100302088
8. A. Dey, "Semiconductor metal oxide gas sensors: A review," Materials Science and Engineering: B, vol. 229, pp. 206–217, Mar. 2018. doi: 10.1016/j.mseb.2017.12.036
9. Figaro Engineering Inc., "MQ-2 Semiconductor Sensor for Combustible Gas — Technical Information," Figaro USA, Inc., Glenview, IL, 2010. [Online]. Available: https://www.figaro.co.jp
10. Microchip Technology Inc., "ATmega328P 8-bit AVR Microcontroller with 32K Bytes In-System Programmable Flash — Datasheet," Microchip Technology, Chandler, AZ, 2018. [Online]. Available: https://www.microchip.com
11. M. Banzi and M. Shiloh, Getting Started with Arduino, 3rd ed. Sebastopol, CA: O'Reilly Media, 2015. ISBN: 978-1449363338
12. N. Yamazoe and K. Shimanoe, "Theory of power laws for semiconductor gas sensors," Sensors and Actuators B: Chemical, vol. 128, no. 2, pp. 566–573, Jan. 2008. doi: 10.1016/j.snb.2007.07.036
13. S. Das and V. Jayaraman, "SnO_2: A comprehensive review on structures and gas sensors," Progress in Materials Science, vol. 66, pp. 112–255, Oct. 2014. doi: 10.1016/j.pmatsci.2014.06.003
14. P. Bhattacharyya, "Technological journey towards reliable microheater development for MEMS based gas sensor: A review," IEEE Transactions on Device and Materials Reliability, vol. 14, no. 2, pp. 589–599, Jun. 2014. doi: 10.1109/TDMR.2014.2311801
15. G. Korotcenkov and B. K. Cho, "Instability of metal oxide-based conductometric gas sensors and approaches to stability improvement (short survey)," Sensors and Actuators B: Chemical, vol. 156, no. 2, pp. 527–538, Aug. 2011. doi: 10.1016/j.snb.2011.02.024
16. A. Al-Fuqaha, M. Guizani, M. Mohammadi, M. Aledhari, and M. Ayyash, "Internet of Things: A survey on enabling technologies, protocols, and applications," IEEE Communications Surveys and Tutorials, vol. 17, no. 4, pp. 2347–2376, 2015. doi: 10.1109/COMST.2015.2444095
17. International Electrotechnical Commission, IEC 60079-29-1: Explosive Atmospheres — Part 29-1: Gas Detectors — Performance Requirements of Detectors for Flammable Gases, 2nd ed. Geneva: IEC, 2016.
18. Bureau of Indian Standards, IS 8737: Liquefied Petroleum Gas Equipment and Accessories — Specification. New Delhi: BIS, 2012.
19. National Fire Protection Association, NFPA 72: National Fire Alarm and Signaling Code. Quincy, MA: NFPA, 2022.
20. H. Meixner and U. Lampe, "Metal oxide sensors," Sensors and Actuators B: Chemical, vol. 33, no. 1–3, pp. 198–202, Jul. 1996. doi: 10.1016/0925-4005(96)80098-0